



ROMANIAN ACADEMY
“ILIE MURGULESCU” INSTITUTE OF PHYSICAL CHEMISTRY

THESIS SUMMARY
ZnO based ceramic materials with special
properties

Scientific advisor:

Acad. Dr. Maria Magdalena ZAHARESCU

PhD Student:

Maria Cristina VLĂDUȚ

Bucharest 2018

Summary:

I.	INTRODUCTION.....	4
II.	LITERATURE DATA.....	8
II.1.	ZnO OVERVIEW.....	8
II.2.	SYNTHESIS METHODS OF OXIDE COMPOUNDS.....	11
II.2.1.	Solid state reactions.....	11
II.2.2.	Sol-gel method.....	11
II.2.3.	Hydrothermal method.....	14
II.3.	CHARACTERISATION METHODS.....	16
II.3.1.	Scanning Electron Microscopy (SEM).....	16
II.3.2.	X-ray Dispersive Spectroscopy (EDX).....	17
II.3.3.	Transmission Electron Microscopy (TEM).....	17
II.3.4.	Atomic Force Microscopy (AFM).....	18
II.3.5.	X-ray Diffraction.....	19
II.3.6.	Fourier-transform Infrared Spectroscopy (FTIR).....	20
II.3.7.	Thermo gravimetric (TG) and Differential Thermal Analysis (DTA).....	21
II.3.8.	Raman Spectroscopy.....	22
II.3.9.	UV-VIS Spectroscopy.....	23
II.3.10.	X-ray Photoelectron Spectroscopy (XPS).....	23
II.3.11.	Measurements of piezoelectric coefficients.....	24
II.3.12.	References Cap II.....	25
III.	ORIGINAL CONTRIBUTIONS.....	32
III.1.	OBJECTIVES of the THESIS.....	32
III.2.	CHARACTERIZATION TECHNIQUES.....	33
III.2.1.	Films characterization.....	33
III.2.2.	Gels characterization.....	35
III.2.3.	Powders characterization.....	35
III.3.	NANOSTRUCTURED FILMS AND POWDERS IN ZnO BASED SYSTEMS.....	37
III.3.1.	ZnO and Mn doped ZnO films and powders.....	37
III.3.1.1.	ZnO and Mn doped ZnO films obtained by sol-gel method.....	38

III.3.1.1.1. Film preparation.....	38
III.3.1.1.2. Properties of the films obtained by sol-gel method.....	40
III.3.1.2. ZnO and Mn doped ZnO gels and powders obtained by sol-gel method.....	50
III.3.1.2.1. Gels preparation.....	50
III.3.1.2.2. Gels obtained by synthesis.....	50
III.3.1.2.3. Powders obtained by thermal treatment of the gels.....	54
III.3.1.3. ZnO and Mn doped ZnO films obtained by hydrothermal method.....	60
III.3.1.3.1. Film preparation.....	60
III.3.1.3.2. Properties of the films obtained by hydrothermal method.....	63
III.3.1.4. Mn doped ZnO powders obtained by hydrothermal method.....	67
III.3.1.5. Mn doped ZnO films applications.....	73
III.3.1.6. Partial conclusions for Cap.III.3.1.....	75
III.3.1.7. References Cap.III.3.1.....	77
III. 3.2. FILMS AND POWDERS IN ZnO-SnO ₂ SYSTEMS.....	84
III.3.2.1. ZnO-SnO ₂ Films.....	84
III.3.2.1.1. Film preparation.....	85
III.3.2.1.2. Properties of the obtained films.....	87
III.3.2.1.3. Film-based gas sensors in the ZnO-SnO ₂ system.....	91
III.3.2.2. ZnO-SnO ₂ powders.....	95
III.3.2.2.1. Gels preparation.....	96
III.3.2.2.2. Gels obtained by synthesis.....	96
III.3.2.2.3. Powders obtained by thermal treatment of the gels.....	106
III.3.2.2.4. Photocatalytic tests on the ZnO powders.....	110
III.3.2.4. Partial conclusions for Cap.III.3.2.....	112
III.3.2.5. References Cap III.3.2.....	114
IV. CONCLUSIONS.....	117

1. INTRODUCTION

Nanostructured materials, defined as having at least one dimension in the nanometric range (between 1 and 100 nm), enjoyed an increased interest in the community science due to its special and outstanding properties and its various applications as against to bulk material [1-2].

Many potential applications may appear by simply miniaturizing the existing microstructures at a size of 1-100 nm.

Interest in nanostructured materials has increased both in scientific and commercial terms, as they have significant potential in high performance applications. The ceramic industry is no exception, so as to improve the chemical and physical properties of products, the industry increased the demand for nanostructured ceramic materials. Nanoceramics consists of ceramic nanoparticles, generally classified as inorganic solids made of metallic and non-metallic compounds, resistant to high temperatures [3].

The most studied multifunctional material is zinc oxide. This is a n-type semiconductor with wide energy band gap (3.37 eV), large exciton binding energy (60 meV) and high thermal and mechanical stability (at room temperature). It also has low toxicity, biocompatibility and biodegradability, making it attractive for a variety of applications in electronics, optoelectronics, sensors and biomedicine [4-12].

Zinc oxide can easily be obtained in various nanostructured forms, both 1D, 2D and 3D. Thus, the variety of ZnO synthesis methods, such as vapor phase deposition, precipitation, hydrothermal synthesis, sol-gel process, mechanochemical processes, make it possible to produce particles of different sizes, shapes and spatial structures.

It is well known that by introducing a selective element into ZnO lattice the properties of the semiconductor such as band gap or electrical conductivity can be controlled, and in the case of electronic applications the carrier concentration can be increased [13]. Therefore, by tuning its properties ZnO can have novel functionalities, and it can be a promising candidate for diluted magnetic semiconductors (DMS) in which one of the transition metal (TM) ions (e.g. Mn^{2+} , Co^{2+} , Ni^{2+} , and Fe^{2+}) substitutes a fraction of the original atoms from the ZnO host lattice [14].

Taking into consideration the presented considerations, the main objective of this PhD thesis is the study of ZnO 1D and 2D nanostructures with possible applications as sensors, transparent oxide conductors, catalysts or harvesting devices. Also, the correlation of the composition and the method of preparation with the structure, morphology and properties of the obtained nanostructures was investigated.

Thus, the first objective was represented by the synthesis and characterization of ZnO and Mn doped ZnO films and powders obtained by sol-gel method and hydrothermal method.

The second objective was the study of films and powders from the ZnO-SnO₂ binary system obtained by sol-gel method. In this case, in addition to ZnO pure and SnO₂ doped ZnO films, also SnO₂ pure and ZnO doped films were prepared. In addition, a study has been approached to obtain compositions corresponding to the binary compounds mentioned in the literature for this system, namely Zn ortostanate and Zn metastanate.

The thesis is structured in 4 Chapters, as follows:

- Chapter 1 contains general information about nanostructures. The features of 0D, 1D, 2D and 3D type nanostructures are presented.

- Chapter 2 is divided into 3 subchapters. In the first subchapter zinc oxide generalities are presented. The second subchapter presents the main synthesis methods, and in the third subchapter the methods of characterization of the oxidic nanomaterials are presented.

- Chapter 3 contains the most important results obtained in the thesis and is divided into two subchapters: Mn doped ZnO films and powders and ZnO-SnO₂ films and powders.

- Chapter 4 summarizes the general conclusions.

2. ORIGINAL CONTRIBUTIONS

2.1. ZnO AND Mn DOPED ZnO FILMS AND POWDERS

The properties of zinc oxide can be improved by doping it with donor ions, depending on the desired properties and applications. The dopant added to the ZnO nanostructure influences the band gap, as well as the electrical and optical properties of

the oxide [15-18]. Mn doping is very promising, since Mn has the largest number of unbound electrons, and therefore the highest magnetic moment possible [16] and the first half of the “d” band is occupied, which creates a stable, fully polarized state [19]. As a consequence of similar ionic radii of Zn^{2+} (0.074 nm) and Mn^{2+} (0.080 nm), manganese ion can easily be incorporated into the ZnO network without altering its original structure [20]. Mn^{2+} doped ZnO can be prepared by various methods, but most synthesis techniques requires expensive equipment and high temperatures, while the sol-gel method is a simple, low-cost approach in which the composition and homogeneity of films can be easily controlled.

2.1.1. ZnO and Mn doped ZnO films obtained by sol-gel method [21]

The present chapter focuses on the synthesis by sol-gel method and complex characterization of Mn doped ZnO thin films, for several possible applications. Different dopant concentrations were used, namely: 1%, 2%, and 5% Mn. The prepared solutions were deposited on silicon substrates (Si / SiO_x / TiO_2 / Pt) and glass. The technological flow of the films is shown in Figure 1.

The solution was deposited by dip coating (withdrawal speed of 50 mm/min, stationary time in solution 1 minute). To obtain the desired thickness 1-10 layers were deposited. An intermediary thermal treatment of 500°C/5 min was applied after each deposited layer and one final treatment at 500°C/1h.

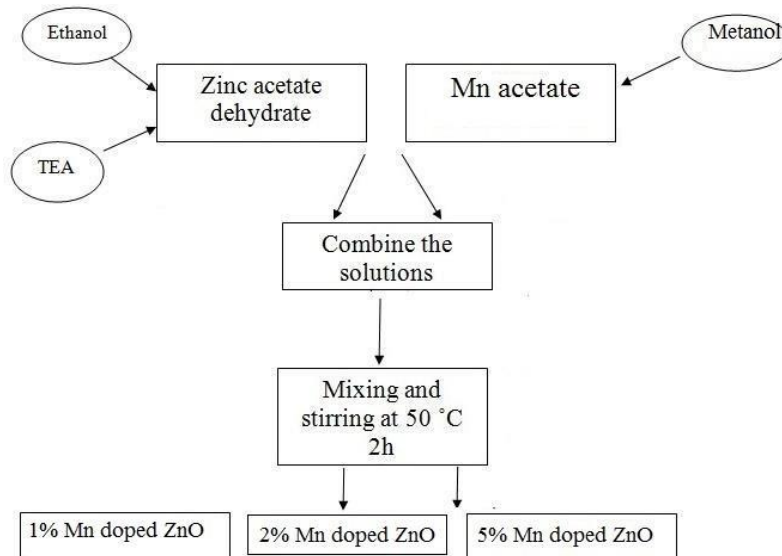


Figure 1. The technological flow of the Mn doped ZnO films

Mn doped ZnO films are continuous, homogeneous, without defects (such as cracks or peeling) and have a nanometer-sized granular morphology with low surface roughness (3-4 nm). The films are polycrystalline, made up of a single layer of echiaxed nanoparticles with diameters of approximately 50 nm (Figure 2).

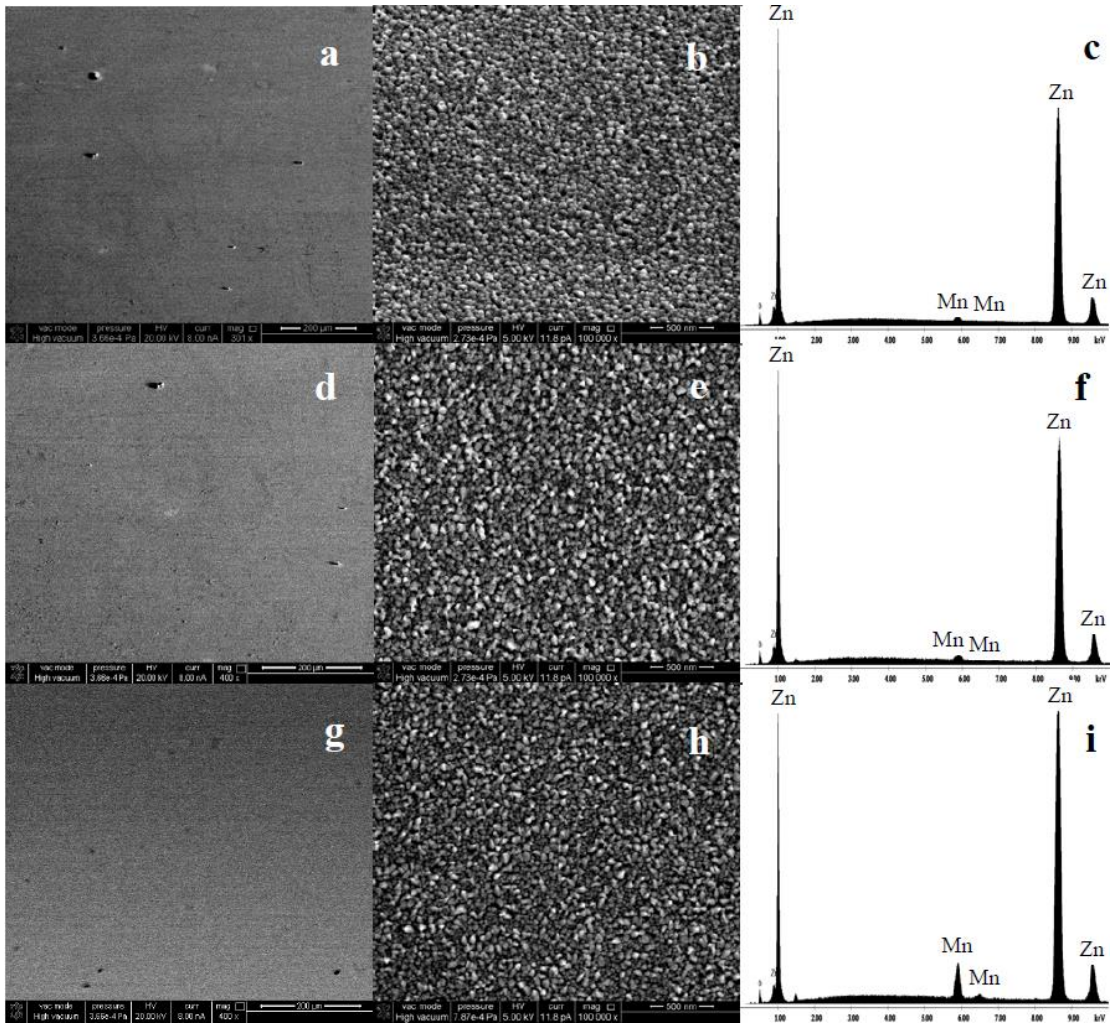


Figure 2: SEM images and EDX spectrum of doped ZnO films prepared by SG after 10 depositions: Mn(1%)(a-c); Mn(2%) (d-f); Mn(5%)(g-i)

EDX analysis detected the dopant presence even for the sample with the smallest Mn (1%), and XRF confirms that the amount of Mn found in the film is in agreement with the amount introduced in synthesis.

The XRD diffractograms (Figure 3) evidence the presence of zincite phase, ZnO, according to ICDD file no. 00-036-1451. Zincite has wurtzite structure, with hexagonal close packing, belonging to hexagonal crystal system, and P63mc (186) space group. No

manganese based compounds were detected within the detection limits of the instrument. This observation suggests that the films are single phase ZnO, with manganese ions incorporated in the zincite structure, as dopants, without changing the hexagonal wurtzite structure.

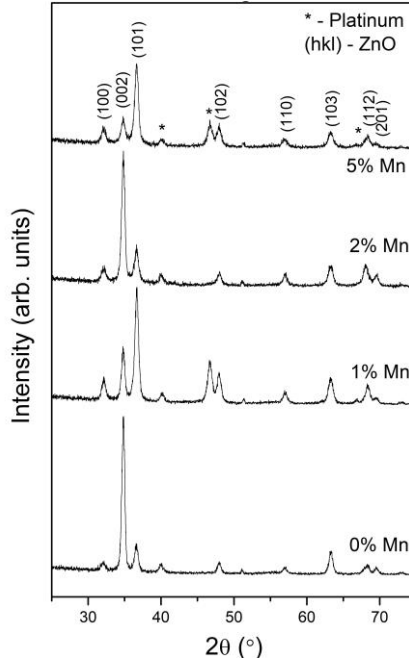


Figure 3. XRD diffractograms of ZnO and Mn doped ZnO films

The refractive index increases with the Mn content, proving a film densification with dopant insertion and a very slow decrease of the band gap (Figure 4).

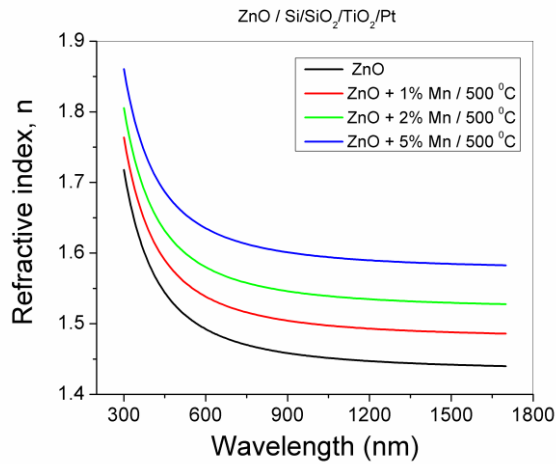


Figure 4. Effect of dopant amount on the refractive index for ZnO films

2.1.2. ZnO and Mn doped ZnO gels and powders obtained by sol-gel method [22]

ZnO and ZnO gels doped with Mn^{2+} (1, 2, 5 at%) resulted from the gelling of the solutions obtained in the preparation of the films, and the powders were obtained by thermal treatment of the gels.

In the case of Mn^{2+} doped ZnO samples there is a similar thermal behavior for all the studied compositions, presenting two main effects: the endothermic effect from about 300°C attributed to the decomposition of Mn hydroxyacetate, and the exothermic effect from above 420°C which is attributed to the oxidation of the organic residues as well as to the crystallization of Mn^{2+} doped ZnO (Figure 5).

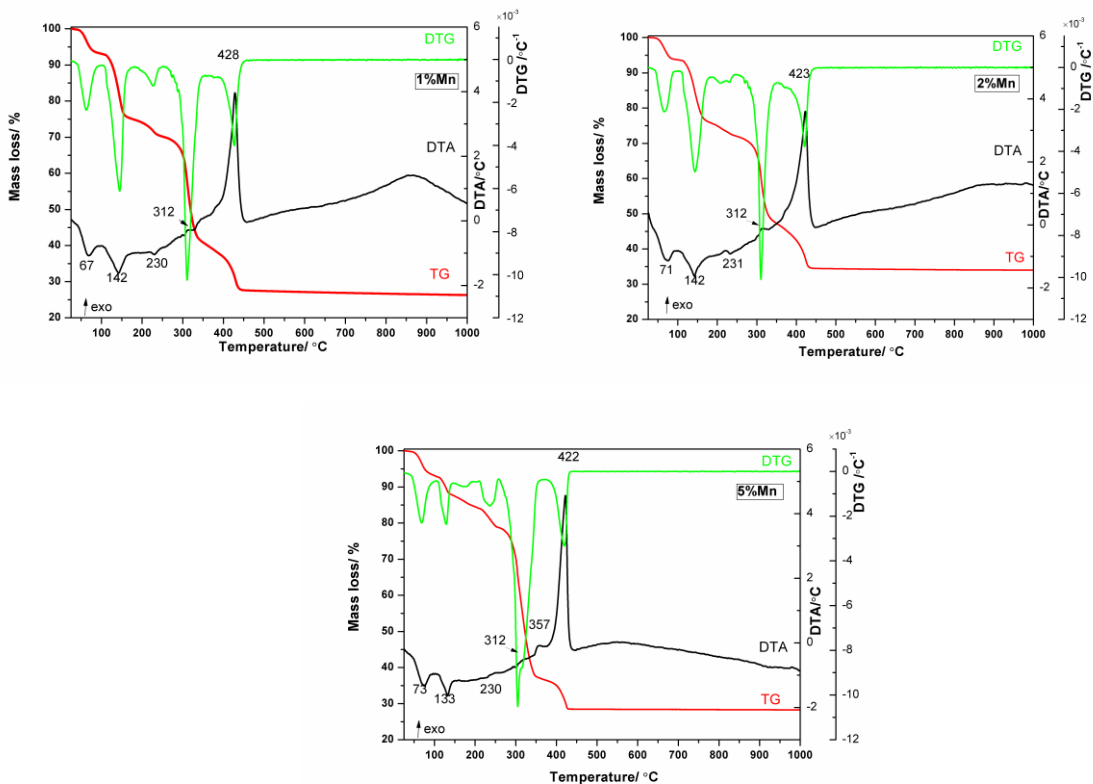


Figure 5. TG/ DTA of the Mn^{2+} doped ZnO: a) 1% Mn, b) 2% Mn, c) 5% Mn

Based on the results obtained by thermal analysis, the samples were thermally treated at 500 °C for one hour, with a heating rate of 5°C/min, in order to obtain Mn^{2+} doped ZnO nanopowders with desired structure and properties.

XRD analysis (Figure 6) showed that all samples had hexagonal wurtzite structure, and the increase in the lattice parameters in Mn^{2+} doped ZnO samples indicated that Mn^{2+} ions substituted Zn^{2+} ions. A decrease of crystallite size with Mn^{2+} addition was highlighted by both X-ray diffraction and scanning electron microscopy. This is due to the decrease of diffusion rate of Mn^{2+} in ZnO.

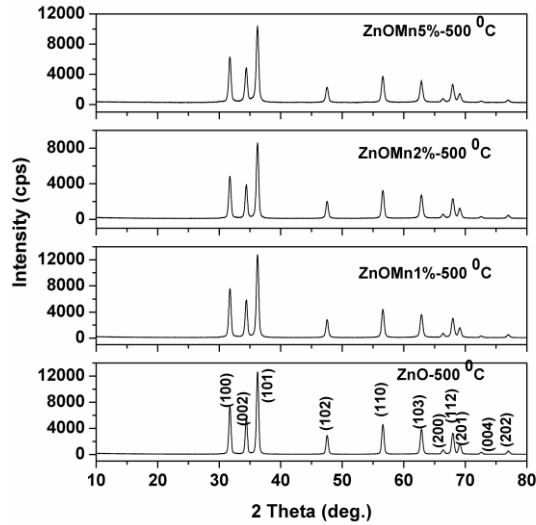


Figure 6. XRD patterns of the ZnO and Mn^{2+} doped ZnO powders

The morphology of the samples depends on Mn^{2+} concentrations, and consists in nanorods with hexagonal cross section, varying their length from 30 to 300 nm (Figure 7).

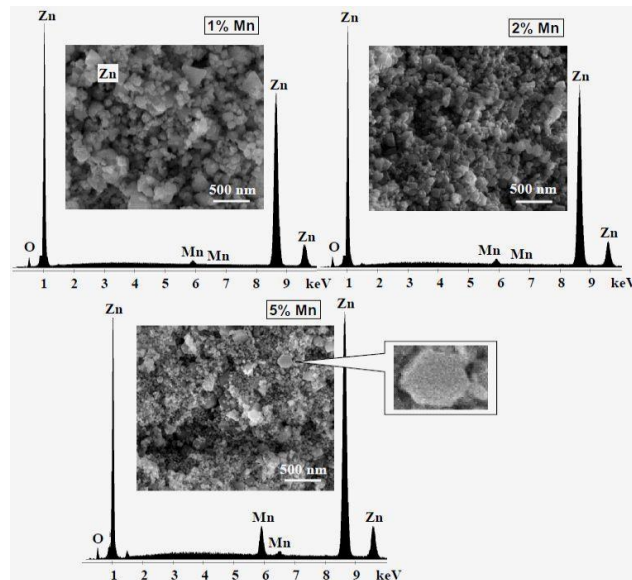


Figure 7. SEM/EDX images of the Mn^{2+} doped ZnO samples

FT-IR spectra (Figure 8) of the powders showed a band at 421 cm^{-1} which is not present in the ZnO spectrum and can be attributed to the Mn-O-Zn bond. Its intensity decreases from ZnO+5%Mn to ZnO+2%Mn and can be correlated with the crystallinity of the samples. In addition, both Raman and EDX spectroscopy confirmed the incorporation of Mn^{2+} into the ZnO lattice.

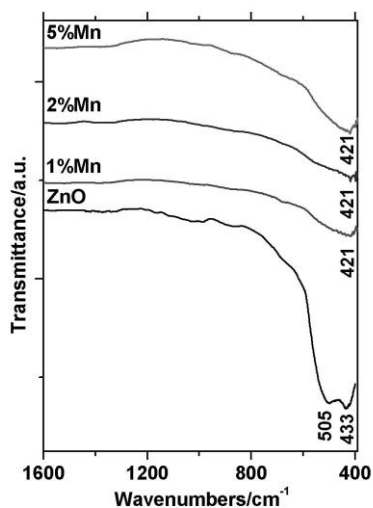


Figure 8. FT-IR spectra of the ZnO and Mn^{2+} doped ZnO powders

2.1.3. ZnO and Mn doped ZnO films obtained by hydrothermal method [21]

The hydrothermal process has several advantages over other growth processes, such as: it is environmentally friendly and less dangerous, simple equipment can be used, large uniform surfaces can be obtained, the method requires no catalysts and has a low cost. This method is attractive for microelectronics because of its reduced temperature reaction [23]. Particle properties, such as morphology and size, can be controlled by hydrothermal process by adjusting the reaction temperature, time and concentration of the precursors.

Zinc aqueous solutions exhibit very low adhesion to the Pt/TiO₂/SiO₂/Si support, especially to the Pt (interest) layer in the hydrothermal bath. In order to obtain zinc oxide nanostructures in the hydrothermal bath, two steps are required. In a first step, a nucleation layer (seed layer) adhering to the Pt surface of the support is deposited by the sol-gel method. The second step consisted in the hydrothermal deposition of the

ZnO_{SG}/Pt/TiO₂/SiO₂/Si plates (in which ZnO_{SG} is the sol-gel seed layer) by transferring them into the teflon cells of the steel autoclave together with the hydrothermal solution.

Mn doped ZnO films obtained by hydrothermal method have a homogeneous morphology, and consists of uniform 1D nanoparticles having a diameter of about 30 nm and lengths of 200-300 nm, being thicker (by an order of magnitude) than those obtained by sol-gel method (Figure 9).

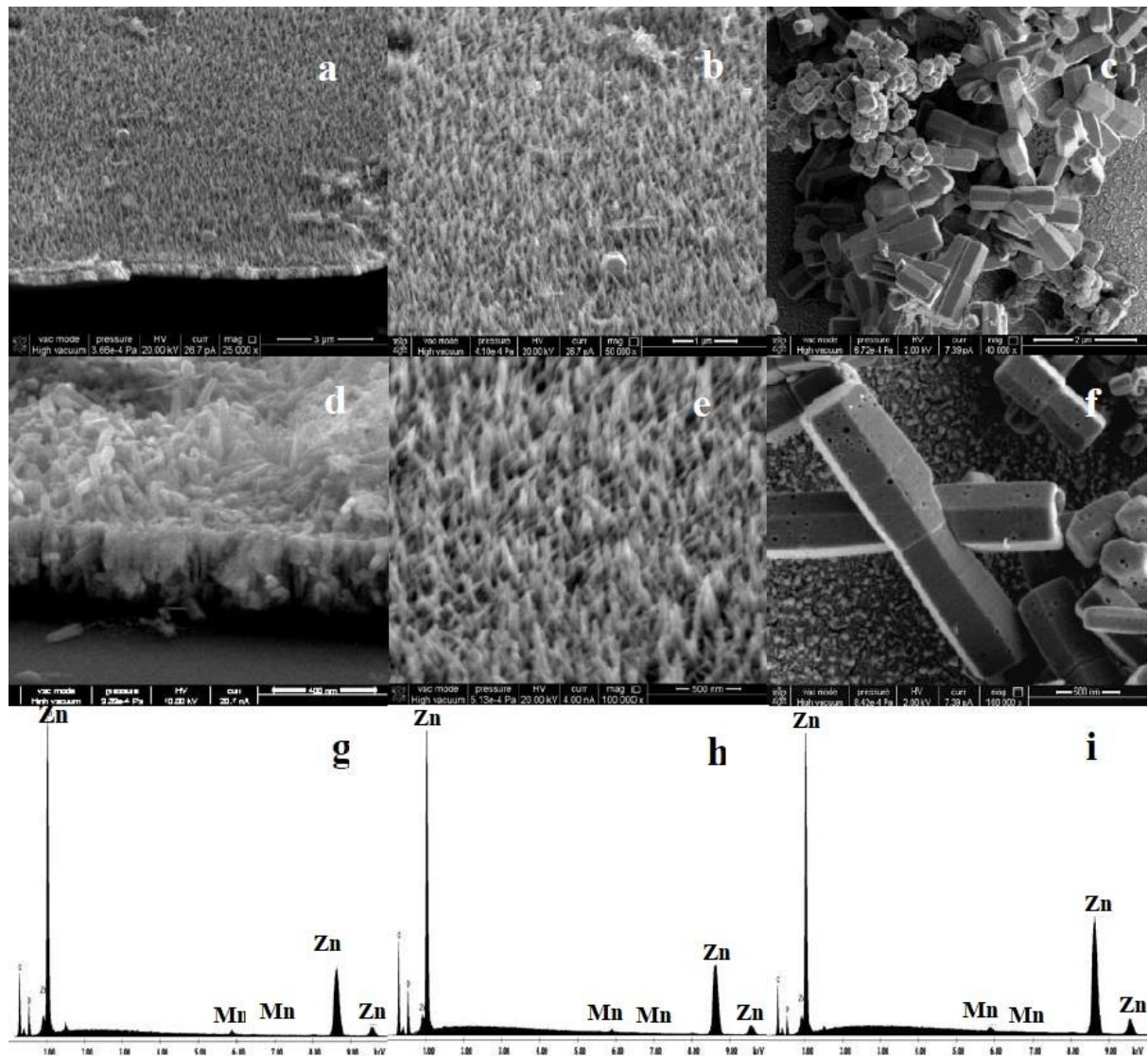


Figure 9. SEM images of Mn doped ZnO (a, b, d, e) and nanorods (c, f) and EDX spectra for: (g) Mn(1%) ; (h) Mn(2%); (i) Mn(5%).

EDX analysis detected the presence of dopant in films, and XRF confirms that the amount of Mn found in the films is in good agreement with the amount introduced in the reaction mixture.

The thin films prepared by hydrothermal method (Figure 10) present a stronger tendency for the crystallites to be oriented along (002) plane (c-axis), but less oriented for 5 at% Mn doped ZnO sample, which is associated with the lattice disorder and strain induced in the ZnO lattice by the substitution of Zn^{2+} ions to larger ionic radius of Mn ions [24].

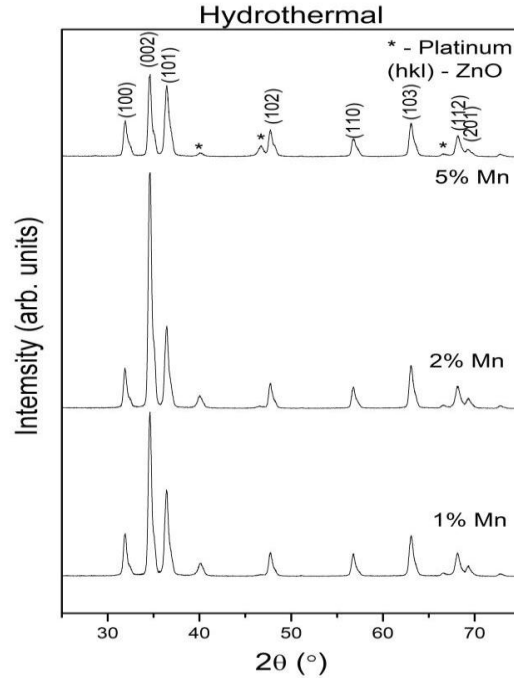


Figure 10. XRD diffractograms of Mn doped ZnO films

2.1.4. Mn doped ZnO powders obtained by hydrothermal method

Hydrothermal powders were obtained by filtering the solutions used to obtain thin films, and drying the resulting precipitate at 100 °C/12 h. These were characterized by FTIR spectroscopy, X-ray diffraction, scanning electron microscopy and thermal analysis.

The powders showed an advanced degree of crystallinity according to X-ray diffraction (Figure 11) and the TG/DTA curves (Figure 12) revealed the thermal behavior of the samples, exhibiting only one endothermic effect, which is attributed to the decomposition of the hydroxyzincite, the secondary phase present alongside the majority component, zincite.

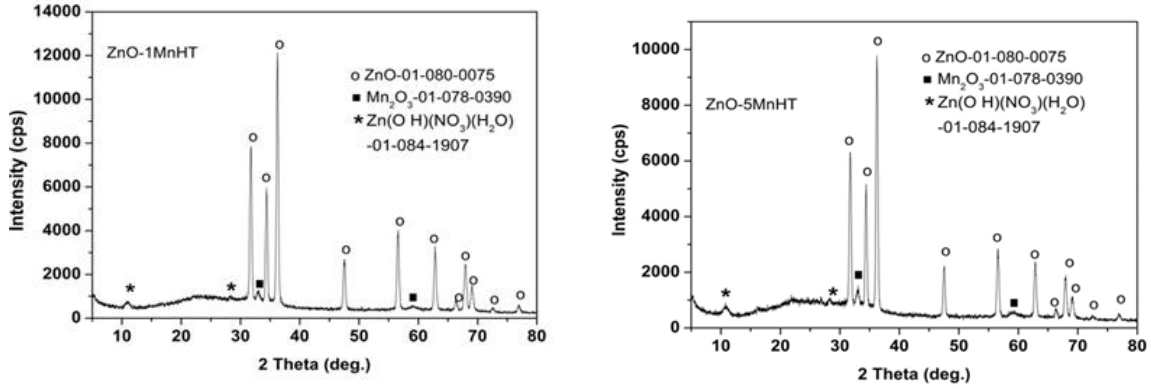


Figure 11. XRD diffractograms of : (a) 1% , (b) 5% Mn doped ZnO

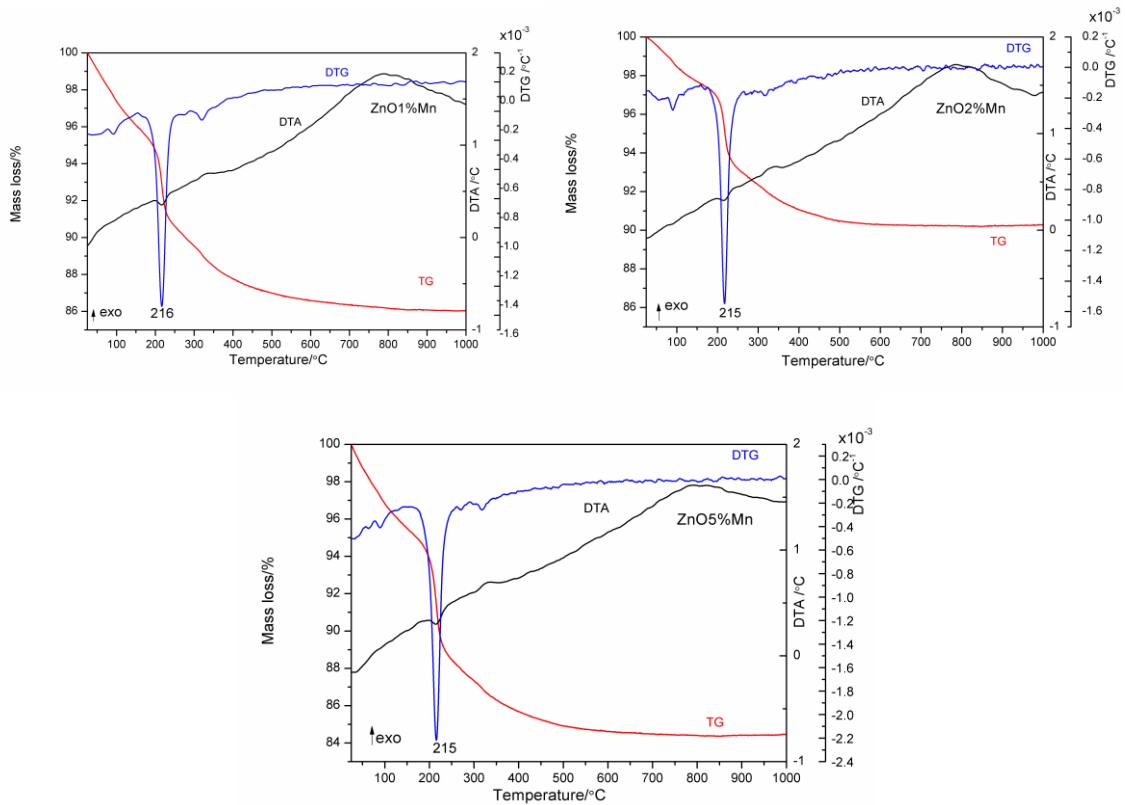


Figure 12. TG/DTA of the Mn^{2+} doped ZnO: a) 1% Mn, b) 2% Mn, c) 5% Mn

2.1.5. Mn doped ZnO films application [21]

The piezoelectric properties of ZnO can be improved by doping with Mn ions. For the films obtained by the sol-gel method and by the hydrothermal method, preliminary tests were performed to highlight the presence of this property.

In Figure 13 it can be observed that the largest piezoelectric effect was obtained for the hydrothermal films, especially for the 2 at%Mn doped sample. Most probably, the largest values of d_{33} obtained for the samples prepared by HT, could be related to the presence of $Mn^{3+/4+}$ inside the ZnO matrix, which is essential for the obtaining of a significant piezoelectric effect [25]. Oxidation of Mn^{2+} (from the reagent used) to $Mn^{3+/4+}$ from the aqueous solution used in the HT preparation method it's also mentioned in the literature [26].

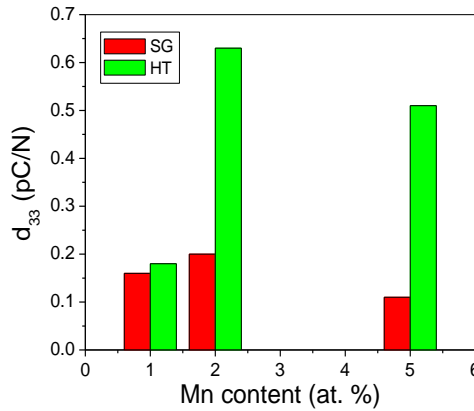


Figure 13. d_{33} parameter, measured on the Mn^{n+} doped films

2.2. FILMS AND POWDERS IN THE ZnO-SnO₂ SYSTEM

Studies on obtaining the binary SnO₂-ZnO oxide materials are of interest because SnO₂ improves the properties of ZnO resulting in materials with excellent optical properties and high performance in detecting gases [27-30].

SnO₂ is a n-type direct wide-band semiconductor, and is transparent in the visible light region [31].

Used as transistor it has high thermal conductivity, excellent mechanical properties and a simple microstructure [32]. It is used as a gas sensor because of its high sensitivity, fast response and stability of parameters [33].

2.2.1. ZnO-SnO₂ films [34]

In this chapter ZnO-SnO₂ thin films were obtained and can be used for developing a gas sensor with selectivity for CO even in small quantities (5 ppm). For this purpose,

the detection layer was deposited by dip-coating method using solutions obtained by sol-gel method.

All samples had an amorphous structure (Figure 14), and the film's sensitive layer showed high transparency. The sample S2 (containing 2% SnO₂ and 98% ZnO) had a very high porosity, facilitating the absorption of gas on the surface, thus improving the sensory properties of the studied material.

The obtained sensors were tested by exposure to various gases: C₃H₈, CH₄, CO₂ and CO. Sensor S2 exhibited the highest CO response of up to 5 times greater than that of pure ZnO, having in the same time good selectivity. While sensor S4 (containing 2% ZnO and 98% SnO₂) showed a high humidity response at room temperature.

The response time of sensor S2 was 120 seconds, and its full recovery was achieved in a maximum of 280 seconds. One year after the sensitive layer was deposited (October 2015 - Oct 2016), it was found that the S2 sensor still gives responses, even at low CO concentrations (5 ppm), at a working temperature of 300 °C. Although the working temperature has increased from 210 to 300°C, the film has shown stability over time.

Since the results are reproducible, the preparation method can be proposed for use on a large scale (Figure 15).

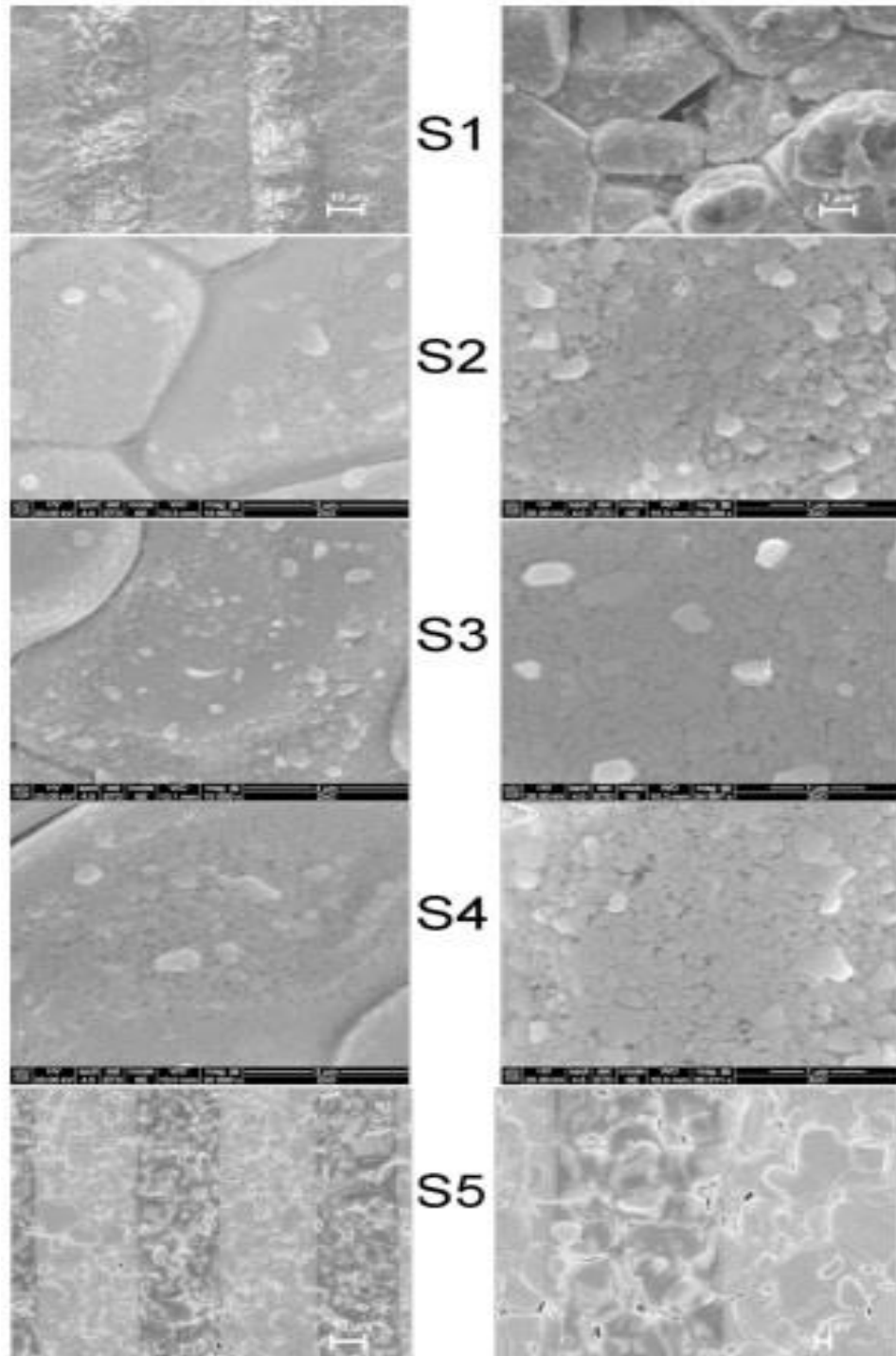


Figure 14. SEM images of S1-S5 samples

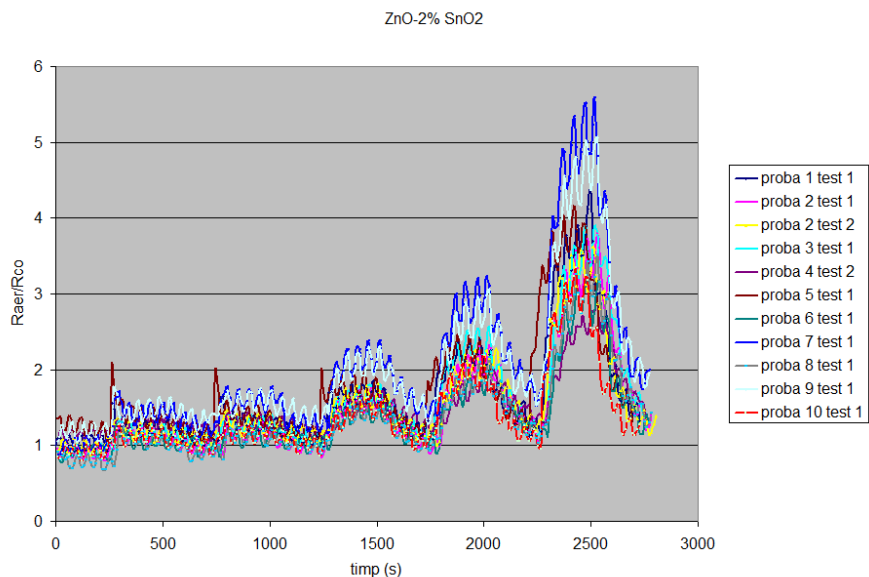


Figure 15. Reproducibility of the samples

2.2.2. ZnO-SnO₂ powders [35]

The solutions used for the preparation of films in the ZnO-SnO₂ system were stored at room temperature in air and left for gelling. The gels were thermally, morphologically and structurally studied in order to determine the optimal conditions of thermal treatment and phase formation in the binary system. Thus, gels and powders of tin oxide, zinc oxide and binary samples with a Sn: Zn = 1: 1 molar ratio, and Sn: Zn = 1: 2 were obtained.

XRD and FTIR analyzes (Figure 16 and Figure 17) showed that the prepared samples were amorphous. The XRD pattern of pure ZnO dried at 100 °C reveals the presence of ZnO mixed with anhydrous zinc acetate and hydroxyzincite. With the help of these investigations, the rutile structure for SnO₂ and the wurtzite type for ZnO was established.

The thermal behavior of the gels was investigated using the TG/DTA-MS method in air atmosphere and in nitrogen. Only endothermic effects occurs in the air at temperatures up to 300 °C. In the temperature range 300-500 °C, the exothermic effects due to the oxidation of the organic part and the crystallization of the oxidic compounds were observed. In the case of nitrogen atmosphere only endothermic effects occur (Figure 18).

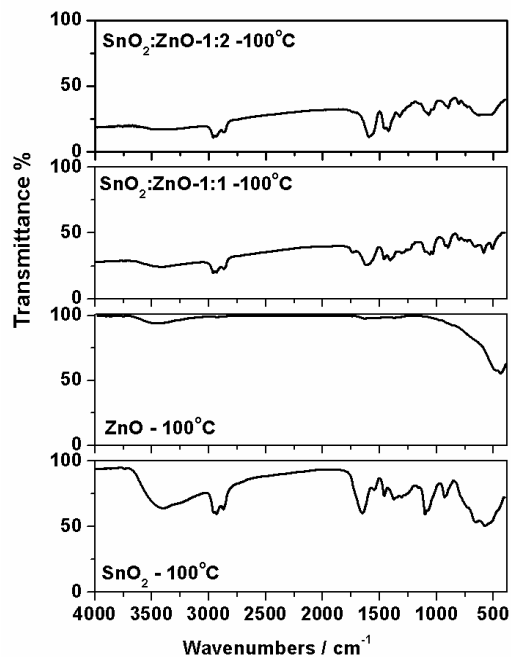


Figure 16. FTIR spectra of dried gels at 100°C

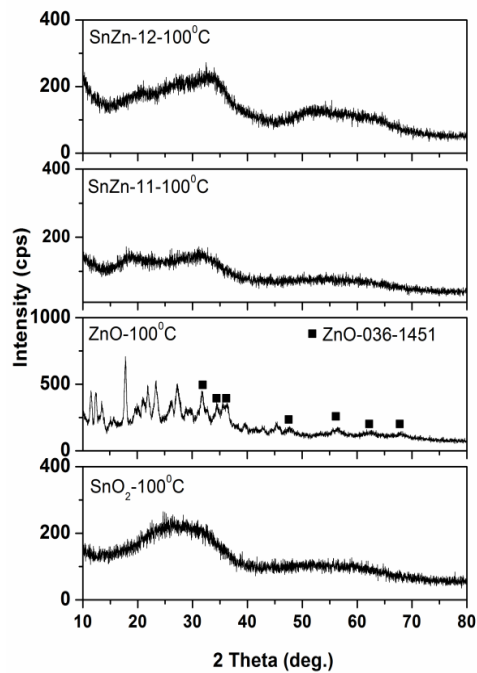


Figure 17. XRD patterns of the as prepared samples dried at 100 °C

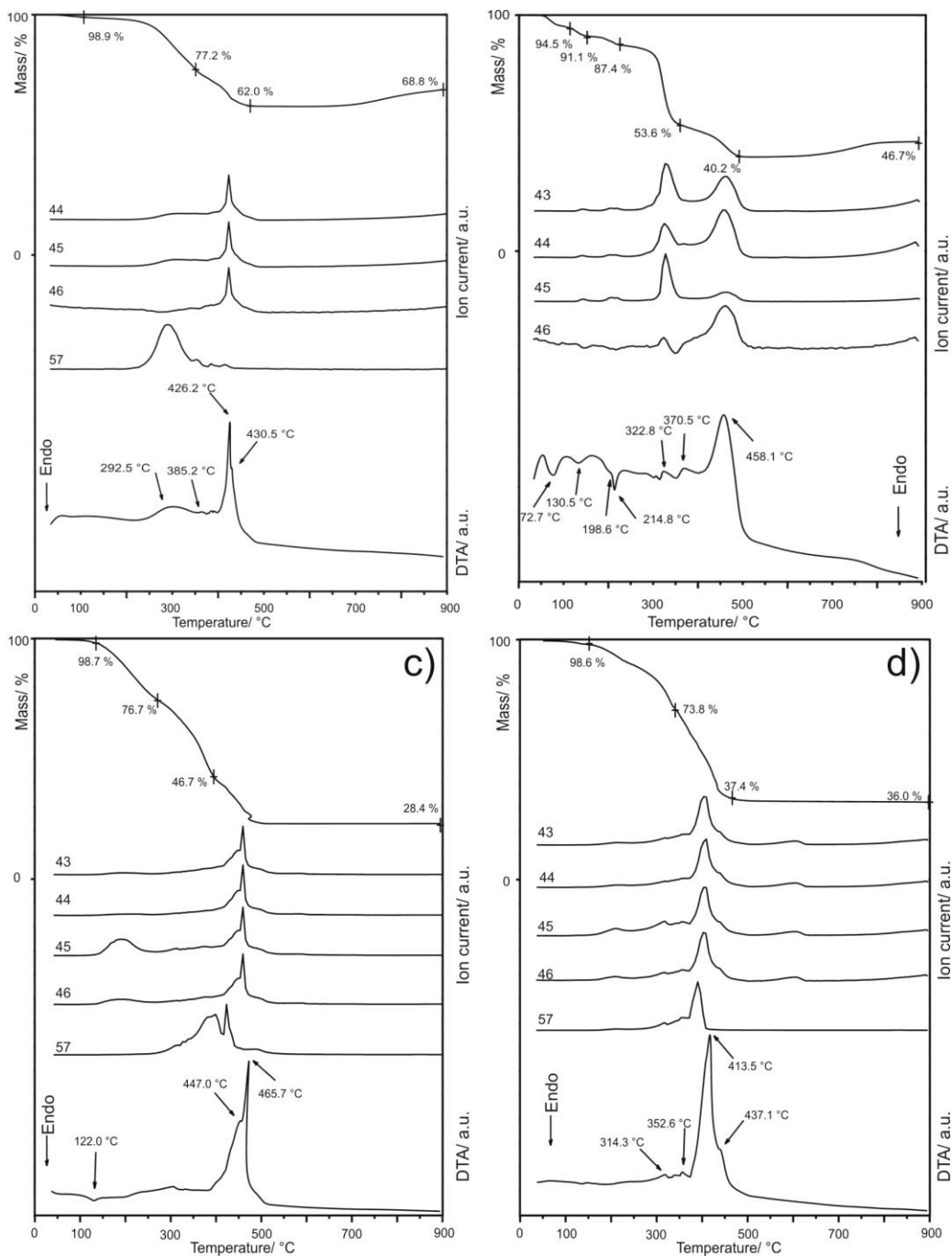


Figure 18. TG/DTA-MS curves of the gels analyzed in air: a) SnO_2 , b) ZnO , c) SnO_2 - ZnO 1:1, d) SnO_2 - ZnO 1:2

The morphologic characterization of the iso-thermally treated samples at 500 °C performed by SEM is presented in Figure 19. Each sample possesses a different morphology due to their different composition. While SnO_2 grains are relatively large the ZnO sample presents smaller grains and the morphology appears clearly more compact,

with less interparticle voids. The sample with Sn:Zn = 1:1 molar ratio presents a combination of smaller grains (ZnO) and bigger grains (SnO₂), as for Sn:Zn = 1:2 molar ratio the morphology revealed that the coalescence of the grains led to the formation of an “almond-like” grain shape.

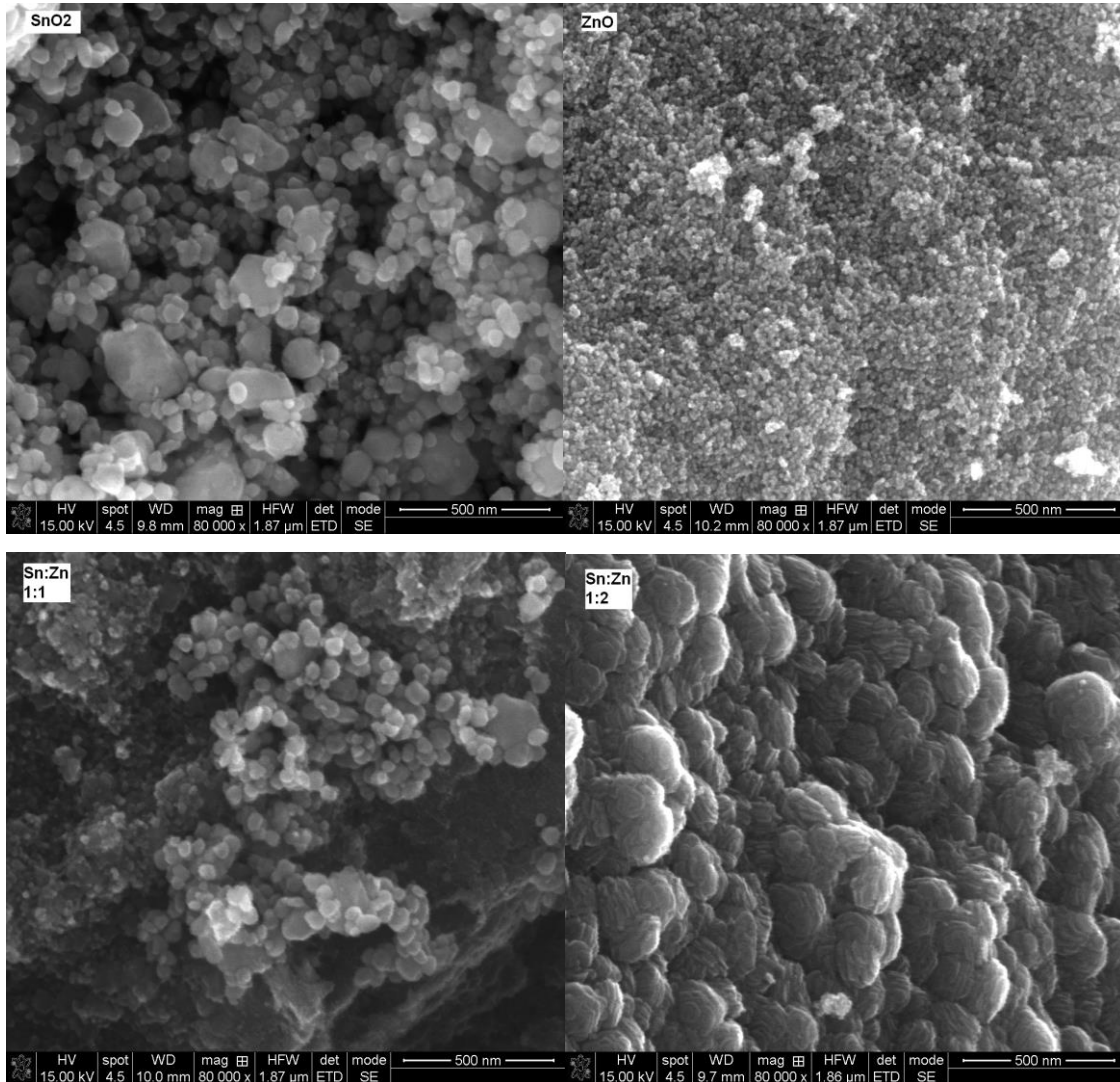


Figure 19. SEM images of the iso-thermally treated samples at 500°C, in air

In the binary SnO₂-ZnO samples for both studied compositions the zinc ortostannate Zn₂SnO₄ was identified, beside different amount of SnO₂. The formation of zinc metastannate ZnSnO₃ was not identified, showing that the used synthesis method probably does not fulfill the conditions for its preparation.

2.2.3. Photocatalytic tests of ZnO powders [36]

Photocatalytic tests of ZnO in the degradation of Rhodamine B had similar values to those of TiO₂, being promising for its use as a photocatalyst (Figure 20).

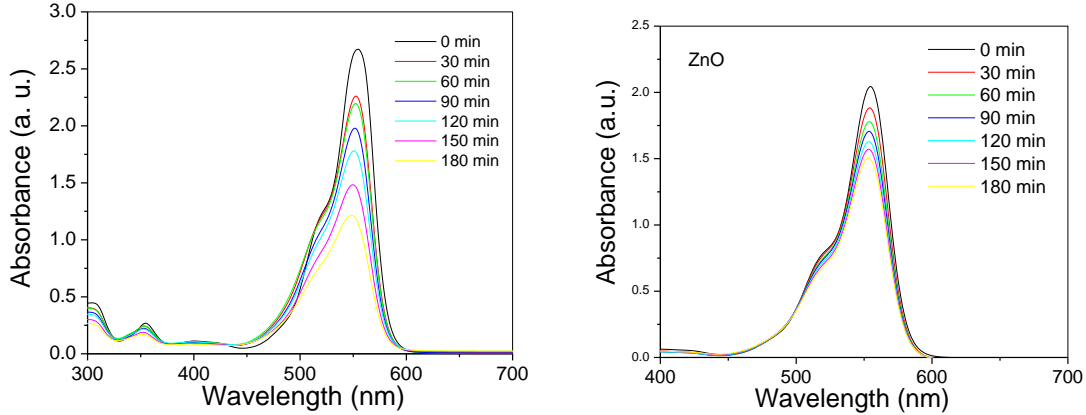


Figure 20. Photocatalytic activity of: (a) TiO₂ and (b) ZnO

3. CONCLUSIONS

In this thesis, researches regarding the obtaining of nanostructures (films and powders) were made in ZnO based systems, using the sol-gel method and the hydrothermal method.

The first objective was to obtain ZnO and Mn doped ZnO films and nanopowders followed by morphological and structural characterization of the samples.

ZnO pure and Mn doped films obtained by the sol-gel method have a homogeneous and continuous morphology, and EDX analysis detected the dopant even for the smallest Mn content sample.

ZnO and Mn doped ZnO gels resulted from the gelling of solutions used for the film preparation. Based on the TG/DTA results, the gels were thermally treated at 500 °C for one hour, in order to obtain nanopowders with desired structure and properties.

In the case of powders, the incorporation of Mn²⁺ into ZnO lattice on the Zn²⁺ position was confirmed by Raman spectroscopy, X-ray diffraction and EDX; and scanning electron microscopy. X-ray diffraction revealed the decrease of the grain size with the increase of Mn²⁺ concentration due to the decrease of diffusion rate in ZnO.

Mn doped ZnO films obtained by hydrothermal method also have a homogeneous morphology, these being thicker in size than those obtained by the sol-gel method. On both type of films, preliminary tests were performed to determine the piezoelectric properties. Due to the higher thickness and due to the fact that Mn^{2+} can be oxidized to $Mn^{3+ / 4+}$ in aqueous solution, hydrothermal films have a higher piezoelectric response than those synthesized by sol-gel.

The second objective was the study of films and nanopowders from the ZnO-SnO₂ binary system obtained by sol-gel method. In this case, in addition to pure ZnO and SnO₂ (2%) doped ZnO films, also pure SnO₂ and ZnO (2%) doped SnO₂ films were prepared. In addition, compositions corresponding to the binary compounds mentioned in the literature for this system, namely Zn orthostanate and Zn metastanate were prepared and investigated.

Tin oxide, zinc oxide and binary samples with Sn:Zn = 1: 1 and Sn:Zn = 1: 2 molar ratio possess a different morphology because of their different composition.

The thermal behavior of the gels was investigated using the TG/DTA-MS method in air atmosphere and in nitrogen.

From the XRD analysis, it was observed that they are amorphous at 100 °C, except for the precursor powder of ZnO. In both binary samples the Zn₂SnO₄ zinc orthostanate formation was identified while the presence of ZnSnO₃ was not observed in the corresponding sample, probably due to the fact that the conditions for its preparation were not met.

The bicomponent films of ZnO-SnO₂ had an amorphous structure with a granular morphology of nanometric dimensions (31.3 nm).

All synthesized composites have been tested as gas and humidity sensors. The S2 sample (2% SnO₂ and 98% ZnO) showed the highest CO response, up to 5 times higher than pure ZnO. This sensor is also exhibiting the highest porosity. For sensor S4 (containing 2% ZnO and 98% SnO₂) a high humidity response at room temperature was obtained.

The obtained results in the thesis were the subject of 6 published papers

Selective references:

1. H.S. Nalwa, Handbook of Nanostructured Materials and Nanotechnology, Acad. Press, New York, 2000
2. J.R. Heath, A special issue on nanoscale materials, Acc. Chem. Res., 1999; 32(5): 387
3. A. Khalil, Advanced Sintering of Nano-Ceramic Materials, Ceram. Mater-Progress in Modern Ceramics, 2012.
4. . Schmidt-Mende, J. L. MacManus-Driscoll, ZnO – nanostructures, defects, and devices, Mater. Today, 2007; 10(5): 40-48
5. J. Pan, H. Shen, S. Mathur, One-Dimensional SnO₂ Nanostructures: Synthesis and Applications, J. of Nanotechnol., 2012; 1-12
6. E. Bacaksiz, M. Parlak, M. Tomakin, A. Özcelik, M. Karakiz, M. Altunbas, The effect of zinc nitrate, zinc acetate and zinc chloride precursors on investigation of structural and optical properties of ZnO thin films, J. Alloy. Compd., 2008; 466: 447-450
7. J. Wang, J. Cao, B. Fang, P. Lu, S. Deng, H. Wang, Synthesis and characterization of multipod, flower-like, and shuttle-like ZnO frameworks in ionic liquids, Mater. Lett., 2005 ; 59: 1405-1408
8. Z.L. Wang, Splendid one-dimensional nanostructures of zinc oxide: A new nanomaterial family for nanotechnology, ACS Nano, 2008; 2: 1987–1992
9. M. Chaari, A. Matoussi, Electrical conduction and dielectric studies of ZnO pellets, Phys. B Condens. Matter, 2012; 407: 3441-3447
10. Ü. Özgür, Y.I. Alivov, C. Liu, A. Teke, M. A. Reshchikov, S. Doğan, V. Avrutin, S.-J. Cho, and H. Morkoç, A comprehensive review of ZnO materials and devices, J. Appl. Phys., 2005; 98, doi:10.1063/1.1992666
11. S. Bhattacharyya, A. Gedanken, A template-free, sonochemical route to porous ZnO nano-disks, Microporous Mesoporous Mater., 2007; 110: 553-559
12. B. Ludi, M. Niederberger, Zinc oxide nanoparticles: Chemical mechanism and classical and non-classical crystallization, Dalton Trans., 2013; 42: 12554-12568

13. R.K. Sharma, S. Patel, K.C. Pargaian, Synthesis, characterization and properties of Mn-doped ZnO nanocrystals, *Adv. Nat. Sci.: Nanosci. Nanotechnol.*, 2012; 3: 035005
14. S.A.Wolf, D.D. Awschalom, R.A. Buhrman, J.M. Daughton, M.L.von Molnar, S. Roukes, A.Y.Chtchelkanova, D.M. Treger, Spintronics: a spin-based electronics vision for the future, *Science*, 2001; 294: 1488-1495
15. T. Rezkallah, I. Djabri, M.M. Koç, M. Erkovan, Y. Chumakov, F. Chemam, Investigation of the electronic and magnetic properties of Mn doped ZnO using the FP-LAPW method. *Chinese J. of Phys.* 2017; 55: 1432-1440
16. X. Chen, X. Jing, J. Wang, J. Liu, D. Song, L. Liu, Fabrication of spindle-like ZnO architectures for highly sensitive gas sensors. *Superlatt. Microstruct.* 2013; 63: 204-214
17. F. Achouri, S. Corbel, L. Balan, K. Mozet, E. Girot, G. Medjahdi, M. Ben Said, A. Ghrabi, R. Schneider, Porous Mn-doped ZnO nanoparticles for enhanced solar and visible light photocatalysis. *Mat. and Design.* 2016; 101: 309–316
18. L.C.K. Liao, J.S. Huang, Energy-level variations of Cu-doped ZnO fabricated through sol-gel processing. *J. Alloys Compd.* 2017; 702: 153–160
19. B.B. Straumal, S.G. Protasova, A.A. Mazilkin, A.A. Myatiev, P.B. Straumal, G. Schutz, E. Goering, B. Baretzky, Ferromagnetic properties of the Mn-doped nanograined ZnO films. *J Appl Phys.* 2010; 108: 073923
20. X.X. Dhruvashi, M. Tanemura, P.K. Shishodia, Ferromagnetism in sol-gel derived ZnO: Mn nanocrystalline thin films. *Adv. Mater. Lett.* 2016; 7(2): 116-122
21. **C.M. Vladut**, S. Mihaiu, E. Tenea, S. Preda, J.M. Calderon-Moreno, M. Anastasescu, H. Stroescu, I. Atkinson, M. Gartner, C. Moldovan, M. Zaharescu, Multifunctional Mn doped ZnO films deposited by Sol-Gel and Hydrothermal Methods, *J. Nanomater.* in process of publication
22. **C.M. Vladut**, S. Mihaiu, O.C. Mocioiu, I. Atkinson, J. Pandele-Cusu, E.M. Anghel, J. M. Calderon-Moreno, M. Zaharescu, Thermal studies of Mn²⁺-doped ZnO powders formation by sol–gel method, *J.Therm. Anal. Calorim*, 2018, 1-9

23. A.R. Reddy, A.N. Mallika, K.S. Babu, K.V. Reddy, Hydrothermal synthesis and characterization of ZnO nanocrystals. *International Journal of Mining, Metallurgy & Mechanical Engineering*, 2015; 3: 52-55
24. R. Karmakar, S.K. Neogi, A. Banerjee, S. Bandyopadhyay, Structural; morphological; optical and magnetic properties of Mn doped ferromagnetic ZnO thin film, *Appl. Surf. Sci.*, 2012; 263: 671–677
25. F. Pan, J.T. Luo, Y.C. Yang, X.B. Wang, F. Zeng, Giant piezoresponse and promising application of environmental friendly small-ion-doped ZnO, *Sci. China Tech. Sci.*, 2012; 55(2): 421–436
26. P. Pascal, *Nouveau traité de Chimie Minerale IX*, Ed. Masson et Cie, Paris, 1958
27. Z.L. Wang, Splendid one-dimensional nanostructures of zinc oxide: A new nanomaterial family for nanotechnology, *ACS Nano*. 2008; 2: 1987–1992
28. M. Chaari, A. Matoussi, Electrical conduction and dielectric studies of ZnO pellets, *Phys. B Condens. Matter*. 2012; 407: 3441-3447
29. Ü. Özgür, Y.I. Alivov, C. Liu, A. Teke, M.A. Reshchikov, S. Dogan, V. Avrutin, S.J. Cho, H. Morkoc, A comprehensive review of ZnO materials and devices, *J. Appl. Phys.* 2005; 98- 041301
30. B. Firtat, C. Moldovan, C. Brasoveanu, G. Muscalu, M. Gartner, M. Zaharescu, P. Chesler, C. Hornoïu, S. Mihaiu, **C. Vlăduț**, I. Dascalu, V. Georgescu, I. Stan, Miniaturised MOX based sensors for pollutant and explosive gases detection, *Sensors Actuat. B*. 2017; 249: 647–655
31. J. Pan, H. Shen, S. Mathur, One-Dimensional SnO₂ Nanostructures: Synthesis and Applications, *J. of Nanotech.* 2012; 2012: 1-12
32. E.N. Dattoli, Q. Wan, W. Guo, Y. Chen, X. Pan, W. Lu, Fully Transparent Thin-Film Transistor Devices Based on SnO₂Nanowires. *Nano Lett.* 2007; 7(8): 2463–2469
33. S.H. Mohamed, SnO₂ dendrites–nanowires for optoelectronic and gas sensing applications, *J Alloys Compd.* 2012; 510: 119–124
34. P. Chesler, C. Hornoïu, S. Mihaiu, **C. Vlăduț**, J. M. Calderon Moreno, M. Anastasescu, C. Moldovan, B. Firtat, C. Brasoveanu, G. Muscalu, I. Stan and M.

- Gartner, "Nanostructured SnO₂-ZnO composite gas sensors for selective detection of carbon monoxide", *Beilstein J. Nanotechnol.* 2016, 7, 2045–2056
35. **C.M. Vladut**, S. Mihaiu, I.M. Szilágyi, T.N. Kovács, I. Atkinson, O.C. Mocioiu, S. Petrescu, M. Zaharescu, Thermal Investigations Of The Sn-Zn-O Gels Obtained By Sol-Gel Method, *J. Therm. Anal. Calorim.*, 2018, 1-10
36. S. Mihaiu, O.C. Mocioiu, L. Predoana, I. Atkinson, S. Preda, **C. Vladut**, E. Tenea, M. Stoica, J. Pandele-Cusu, C. Anastasescu, J.M. Calderon-Moreno, M. Anastasescu, M. Gartner, I. Balint, Pristine and Au-modified ZnO vs. TiO₂ nano-powders prepared by sol-gel: synthesis, structural properties and photocatalytic degradation of rhodamine B, *Rev. Roum. Chim.*, 2018; 63(5-6): 407-417

Key words: ZnO, sol-gel, hydrothermal, nanostructures